[7]Kentfield, J. A. C., "The Influence of Free-Stream Turbulence Intensity on the Performance of Gurney-Flap Equipped Wind-Turbine Blades," *Wind Engineering*, Vol. 20, No. 2, 1996, pp. 93–106.

Exact Leading-Term Solution for Low Aspect Ratio Wings

S. C. Rajan* and S. Shashidhar†
Indian Institute of Technology, Madras 600036, India

Introduction

An exact solution is available for the ideal two-dimensional flow past a flat plate at low angles of attack for which the aspect ratio is infinity. The exact solution is easily worked out for the other extreme case of aspect ratio being zero. In this case the flat plate wing has a finite span and is semi-infinitely long, i.e., has a leading edge, but the trailing edge is at infinity. For this case it comes out naturally that the circulation distribution is elliptic and is independent of the shape of leading edge. In the present work the momentum theorem is used to obtain the expression for the leading-edge suction force as it brings out some subtle features that are not seen when the conservation of energy is applied. Sears[1] also makes use of the momentum theorem for calculating induced drag for a high aspect ratio elliptic wing.

Wing in Translation

Basic Theory and Calculation of the Normal Load

In Fig. 1 a semi-infinitely long flat plate having span length $2b$ and chord length infinity is shown exposed to a uniform stream V_∞ at an angle of attack α. The flat plate can be replaced by a vortex sheet and at the Trefftz plane, since the flow becomes two dimensional, the flowfield is known.

From the two-dimensional theory it is known that

$$\gamma_x(\infty, y) = 2V_\infty y \sin\alpha/\sqrt{b^2 - y^2} \tag{1}$$

where γ_x is the intensity of vorticity at the Trefftz plane. It can be readily verified that it satisfies the no-penetration boundary condition. Far downstream the value of $\gamma_y = 0$, and at the leading edge $\gamma_x = 0$. Hence, as we start at infinity at the port side of the wing and move toward the leading edge, the vortex lines gradually start curving, eventually intersecting the midspan line, turn, and on reaching infinity at the starboard side, become straight (Fig. 1). At any point on the vortex sheet

$$\boldsymbol{\gamma} = \gamma_x \boldsymbol{i} + \gamma_y \boldsymbol{j}$$

Using Bernoulli's equation it is easily shown that the pressure change Δp across the plate is

$$\Delta p = \rho\gamma_y V_\infty \cos\alpha$$

Hence, the total normal load F_z is

$$F_z = \rho V_\infty \cos\alpha \int_{-b}^{b} dy \int_0^\infty \gamma_y \, dx \tag{2}$$

Fig. 1 Flat plate and its corresponding vortex system.

The circulation Γ at a span location y is

$$\Gamma = \int_0^\infty \gamma_y \, dx \tag{3}$$

From Helmholtz's conservation equation it follows that

$$\gamma_x(\infty, y) = -\frac{d\Gamma}{dy} \tag{4}$$

Substituting for γ_x from Eq. (1) and integrating Eq. (4) results in

$$\Gamma = 2V_\infty \sin\alpha\sqrt{b^2 - y^2} \tag{5}$$

It is seen that the expression for Γ is elliptic. Combining Eqs. (2), (3), and (5) the normal load is obtained as

$$F_z = \pi\rho V_\infty^2 b^2 \sin\alpha \cos\alpha$$

Calculation of the Inplane Suction Force

This is easily worked out considering a cylindrical control volume such that its axis is coincident with the x axis. It has a radius R and its upstream and downstream bounding planes are at distances k_1R and k_2R from the origin, where k_1 and k_2 are positive constants and could be equal. In the following analysis, surfaces 1 and 2 refer to the upstream and the downstream bounding planes, respectively, and 3 refers to the curved cylindrical surface. For estimating the order of magnitude of the velocity and the remaining quantities on the bounding surfaces, the wing is replaced by a single horseshoe vortex.

From the momentum theorem it is known that

$$F_x = -\int_{1+2+3} P \, dS - \int_{1+2+3} \rho V_n u \, dS \tag{6}$$

The contribution of 3 to the momentum integral, which is caused by the combined effect of the trailing vortices and the bound vortex, is first evaluated. Let (x, y, z) be any point on surface 3. The normal velocity V_n to the surface 3 satisfies $V_n(x, y, -z) = -V_n(x, y, +z)$. Also, $u = V_\infty \cos\alpha + u'$, where u' is only caused by the bound vortex and satisfies the relation $u'(x, y, -z) = -u'(x, y, +z)$. Hence, $\int_3 \rho V_n u \, dS$ reduces to $\int_3 \rho V_n u' \, dS$. Now, $V_n = \mathbb{O}(1/R^2)$, $u' = \mathbb{O}(1/R^2)$ and the area of surface 3 is of the $\mathbb{O}(R^2)$ and, therefore, $\int_3 \rho V_n u' \, dS \to 0$ as $R \to \infty$.

Similarly, the combined contribution of planes 1 and 2 to the momentum integral is zero. Hence, there is only the pressure integral contribution to the suction force and Eq. (6) reduces to

$$F_x = -\int (P_{d\infty} - P_{u\infty}) \, dS \tag{7}$$

where $P_{d\infty}$ and $P_{u\infty}$ represent the pressures far downstream and far upstream, respectively. From Bernoulli's equation it follows that

$$P_{d\infty} - P_{u\infty} = -\tfrac{1}{2}\rho[(v'^2 + w'^2) + 2V_\infty \sin\alpha \, w']$$

Received Nov. 25, 1996; revision received Jan. 20, 1997; accepted for publication March 3, 1997.

*Assistant Professor, Department of Aerospace Engineering.
†Research Scholar, Department of Aerospace Engineering.

Fig. 2 Contour on the Trefftz plane for integration.

where v' and w' represent the velocity perturbations in the y and z directions, respectively. From the previous equation and Eq. (7), it follows that

$$F_x = \frac{1}{2}\rho \int_{-\infty}^{\infty}\int_{-\infty}^{\infty} (v'^2 + w'^2)\,dy\,dz + \rho \int_{-\infty}^{\infty}\int_{-\infty}^{\infty} V_\infty \sin\alpha w'\,dy\,dz \tag{8}$$

The first term on the right-hand side (RHS) of Eq. (8) is called E, which is the kinetic energy of the flow per unit distance at the Trefftz plane. Denoting the second term by E', Eq. (8) can be written as

$$F_x = E + E'$$

From Ref. 2 it follows that

$$E = -\rho \oint \phi \frac{\partial \phi}{\partial n}\,ds$$

where ϕ stands for the perturbation potential. Here, the contour integration is to be done over the right side of the plate at the Trefftz plane as shown in Fig. 2. In the previous equation, $\partial\phi/\partial n = \pm V_\infty \sin\alpha$ and $ds = \pm dy$ for the lower and the upper sides, respectively, and hence, it can be written as

$$E = \rho V_\infty \sin\alpha \int_0^b (\phi_u - \phi_l)\,dy \tag{9}$$

where

$$\phi_u - \phi_l = \int_y^b \gamma_x(\infty, \eta)\,d\eta \tag{10}$$

As the next step the expression for E' is considered and can be written as

$$E' = \rho V_\infty \sin\alpha \int_{-\infty}^{\infty} dy \int_{-\infty}^{\infty} \frac{\partial \phi}{\partial z}\,dz$$

which simplifies to

$$E' = 2\rho V_\infty \sin\alpha \int_0^b (\phi_l - \phi_u)\,dy \tag{11}$$

From Eqs. (8), (9), and (11) the expression for the suction force is obtained as

$$F_x = -\rho V_\infty \sin\alpha \int_0^b (\phi_u - \phi_l)\,dy$$

Using Eqs. (4) and (5), Eq. (10) simplifies to

$$\phi_u - \phi_l = 2V_\infty \sin\alpha\sqrt{b^2 - y^2}$$

Fig. 3 Stationary and rotating coordinate systems.

The expression for the suction force is finally given by

$$F_x = -\tfrac{1}{2}\pi\rho V_\infty^2 b^2 \sin^2\alpha$$

from which the lift force is

$$L = \pi\rho V_\infty^2 b^2 \sin\alpha \cos^2\alpha + \tfrac{1}{2}\pi\rho V_\infty^2 b^2 \sin^3\alpha$$

and the induced drag is

$$D_i = \tfrac{1}{2}\pi\rho V_\infty^2 b^2 \sin^2\alpha \cos\alpha$$

Wing in Roll

In this case the plate is exposed to a uniform stream V_∞ and is rotating with an angular velocity of $\boldsymbol{\omega} = \omega \boldsymbol{i}$. The angle of attack is zero. It can be verified that for this case

$$\gamma_x(\infty, y) = -\omega(2y^2 - b^2)/\sqrt{b^2 - y^2}$$

Using Eq. (4), Γ is obtained as

$$\Gamma = -\omega y\sqrt{b^2 - y^2} \tag{12}$$

Hence, the moment to be applied is

$$M = \tfrac{1}{8}\pi\rho V_\infty \omega b^4$$

The expression for the suction force is obtained from the momentum theorem and is given by Eq. (7). Since the flow is unsteady, from Bernoulli's equation the expression for the pressure difference is obtained as

$$P_{d\infty} - P_{u\infty} = -\rho \frac{\partial \phi}{\partial t} - \frac{1}{2}\rho(v'^2 + w'^2) \tag{13}$$

The expression for $\rho(\partial\phi/\partial t)$ is worked out as follows. In Fig. 3 the rotating plate is shown at the Trefftz plane. Let the velocity potential in the plate fixed coordinates Y and Z be $\Phi(Y, Z)$. The transformation equations for the new coordinate system is

$$\begin{aligned} Y &= y\cos\omega t + z\sin\omega t \\ Z &= -y\sin\omega t + z\cos\omega t \end{aligned} \tag{14}$$

Since $\phi(x, y, t) = \Phi(Y, Z)$, it follows that

$$\frac{\partial \phi}{\partial t} = \frac{\partial \Phi}{\partial Y}\frac{\partial Y}{\partial t} + \frac{\partial \Phi}{\partial Z}\frac{\partial Z}{\partial t}$$

Using Eq. (14), the previous equation at $t = 0$ simplifies to

$$\frac{\partial \phi}{\partial t} = \frac{\partial \phi}{\partial y}\omega z - \frac{\partial \phi}{\partial z}\omega y$$

From Eqs. (7) and (13) the expression for the suction force F_x is obtained as

$$F_x = \rho \int_{-\infty}^{\infty}\int_{-\infty}^{\infty} \left[\left(\frac{\partial \phi}{\partial y}\omega z - \frac{\partial \phi}{\partial z}\omega y\right) + \frac{1}{2}(v'^2 + w'^2)\right] dy\,dz \tag{15}$$

The first term on the RHS of the previous equation is

$$\int_{-\infty}^{\infty} dz \int_{-\infty}^{\infty} \omega \frac{\partial \phi}{\partial y}\, dy = 0$$

$$\int_{-\infty}^{\infty} y\, dy \int_{-\infty}^{\infty} \omega \frac{\partial \phi}{\partial z}\, dz = \int_{-b}^{b} \omega y(\phi_1 - \phi_u)\, dy$$

The second term in Eq. (15) is E, the kinetic energy of the flow per unit distance at the Trefftz plane, and is shown to be

$$E = -\rho \int_0^b \omega y(\phi_u - \phi_l)\, dy$$

Hence, the expression for the suction force given by Eq. (15) simplifies to

$$F_x = \rho \int_0^b \omega y(\phi_u - \phi_l)\, dy = -\frac{\pi \rho \omega^2 b^4}{16}$$

It can be verified that the same expression for the suction force is obtained from the conservation of energy.

Discussion and Conclusions

From the foregoing analysis it is seen that the expressions obtained for the normal and suction forces are exact. These results do not depend on the planform shape. In particular the circulation distribution is elliptic and does not depend on the shape of the leading edge. It is worthwhile mentioning that the same results were obtained by Jones in his theory of low aspect ratio wings by treating the crossflow past a triangular wing to be approximately two dimensional. For the cases considered in the present work, the aspect ratio of the wing is zero, and hence, this analysis gives the leading term in an asymptotic expansion for small aspect ratio wings.

References

[1]Sears, W. R., "On Calculation of Induced Drag and Conditions Downstream of a Lifting Wing," *Journal of Aircraft*, Vol. 11, No. 3, 1974, pp. 191, 192.

[2]Milne-Thompson, L. M., *Theoretical Hydrodynamics*, 5th ed., Macmillan, New York, 1968, p. 95.

Effect of Angle of Attack on Roll Characteristics of 65-Degree Delta Wing

Lars E. Ericsson*
Mt. View, California 94040

Introduction

FOR aircraft with highly swept wing leading edges the high-alpha aerodynamics are dominated by the effects of vortex breakdown. This Note describes the physical flow processes causing the observed large effect of angle of attack on the roll–trim characteristics of a 65-deg delta wing.

The experimental results[1] in Fig. 1 for a 65-deg delta wing show that when the inclination σ of the roll axis was increased from 30 to 35 deg the delta wing lost its stable trim point at zero roll angle. The multiple roll–trim characteristics for σ = 30 deg have been analyzed extensively,[2–7] whereas very little has been published for other σ values. In the case of σ = 30 deg, the rapid aft movement of vortex breakdown on the leeward wing-half[1] (Fig. 2a), when represented by a discontinuous, jumpwise movement,[5–7] resulted in the idealized characteristics shown in Fig. 3a. The measured $C_l(\phi)$ characteristics, although being highly nonlinear, are continuous rather than discontinuous, with the statically destabilizing data trend starting at $|\phi| = \phi_{cr}$. Figure 2a shows that when $|\phi| > \phi_{cr} \approx 4$ deg, vortex breakdown moves very rapidly toward the trailing edge on the leeward, rising wing-half. The associated statically destabilizing increase of the vortex-induced lift overpowers the statically stabilizing data trend generated by the vortex forward of vortex breakdown,[8] resulting in the measured statically destabilizing $C_l(\phi)$ trend in Fig. 3a for $\phi_{cr} < |\phi| < \phi_d$.

On the right, windward wing-half the vortex breakdown moves steadily forward toward the apex with increasing roll angle because of the associated decrease of the effective leading-edge sweep. The breakdown reaches the apex when $|\phi|$ approaches 14 deg (Fig. 2a). Recent experimental results for a 60-deg delta-wing-body configuration[9] have revealed that a dramatic change of the vortex-induced loads would occur

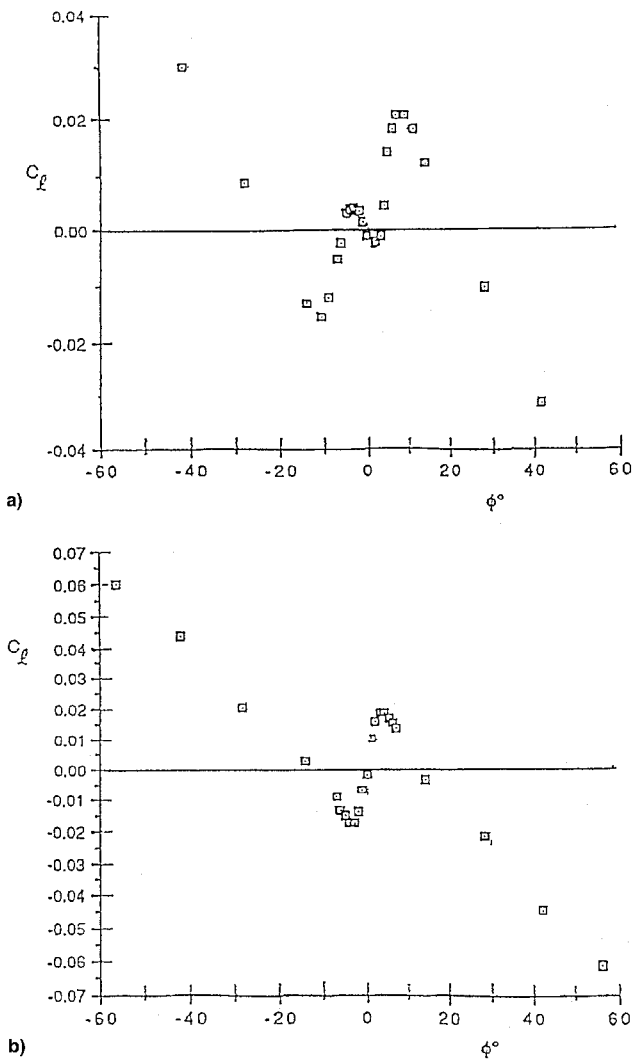

Fig. 1 $C_l(\phi)$ characteristics of 65-deg delta wing.[1] σ = a) 30 and b) 35 deg.

Presented as Paper 96-3443 at the AIAA Atmospheric Flight Mechanics Conference, San Diego, CA, July 29–31, 1996; received Aug. 24, 1996; revision received March 18, 1997; accepted for publication March 19, 1997.

*Engineering Consultant. Fellow AIAA.